Numerical investigation of the sliding response of flexible structures founded on a deformable granular layer

Anastasios Tsiavos[1], Nicholas Alexander[2] and Anastasios Sextos[3]

Abstract

This study focuses on the numerical investigation of the sliding response of flexible structures, simulating school buildings located in Nepal. A deformable granular layer is proposed for the seismic isolation of these structures, aiming at the reduction of their seismic damage. The displacement and acceleration response of the isolated structure is investigated for a wide range of analytical pulse ground motion excitations and one recorded ground motion excitation. The seismic behaviour of the deformable granular layer is compared to the behaviour of a rigid-plastic sliding layer of the same strength. The increased energy dissipation of the deformable sliding layer that emerges from its oscillation before sliding can lead to a significant reduction of the acceleration of the isolated structure.

Keywords: *seismic isolation; granular materials; sliding displacement*

1. Introduction

The sliding response of structures has been widely used in the past as a response modification strategy aiming at the reduction of seismic damage of these structures due to strong earthquake ground motion excitation. However, the effect of the flexibility of the isolated structure and the deformability of the sliding layer on the sliding response of these structures is less well understood. The goal of this study is to quantify the influence of the vibration characteristics of the structure and the granular sliding layer on the sliding response of these structures.

Numerous researchers have investigated the sliding response of a rigid block under harmonic and earthquake ground motion excitation. The response of a sliding block subjected to harmonic excitation has been studied by Westermo & Udwadia (1983) and Mostaghel *et al.* (1983a). Mostaghel *et al.* (1983b) extended this investigation for structures subjected to earthquake ground motion excitation. Castaldo & Ripani (2016) presented an optimization of the design friction of a sliding seismic isolation strategy for different soil conditions.

Kulkarni & Jangid (2003) accounted for the flexibility of the isolated structure and concluded that the difference between the acceleration of a rigid and a flexible isolated structure increases for high values of friction of the seismic isolation system. Vassiliou *et al.* (2013), Tsiavos *et al.* (2017, 2018) and Yaghmaei-Sabegh *et al.* (2018) concluded that designing typical base-isolated superstructures to behave elastically is a necessity that emerges from the dynamics of such structures.

The influence of the elastic stiffness of the sliding interface before sliding commences has been incorporated by Nagarajaiah *et al.* (1991). Nevertheless, this study is mainly focused on Teflon sliding bearing elements, which manifest a significantly stiffer elastic behavior range than the one observed in deformable granular sliding layers. The term granular refers to systems involving a large group of solid particles such as soil, sand, powder, minerals, grains, beads or rocks (Hill & Zeng, 1996). Anthony & Marone (2005) showed that particle characteristics (such as size, shape, and roughness) have a

---
[1] Department of Civil Engineering, University of Bristol, Bristol, United Kingdom, a.tsiavos@bristol.ac.uk
[2] Department of Civil Engineering, University of Bristol, Bristol, United Kingdom, Nick.Alexander@bristol.ac.uk
[3] Department of Civil Engineering, University of Bristol, Bristol, United Kingdom, a.sextos@bristol.ac.uk

remarkable effect on the elastic stiffness, the strength and the particle reorganization within granular materials subjected to sliding deformation.

The combined effect of the elastic stiffness of a granular deformable layer and the flexibility of the isolated structure on the sliding response of structures will be presented in this paper, thus laying the foundation for the design of seismically isolated structures using granular deformable materials. These granular materials could be locally accessible in countries like Nepal, in which the modern, expensive seismic isolation strategies cannot be easily implemented.

2. Dynamic modelling of school buildings in Nepal (SAFER Project)

The sliding response of a flexible structure resembling the dynamic behavior of a low-rise school building founded on a deformable granular layer is simulated using the two-degree-of-freedom model (2 DOF model) shown in Fig. 1.
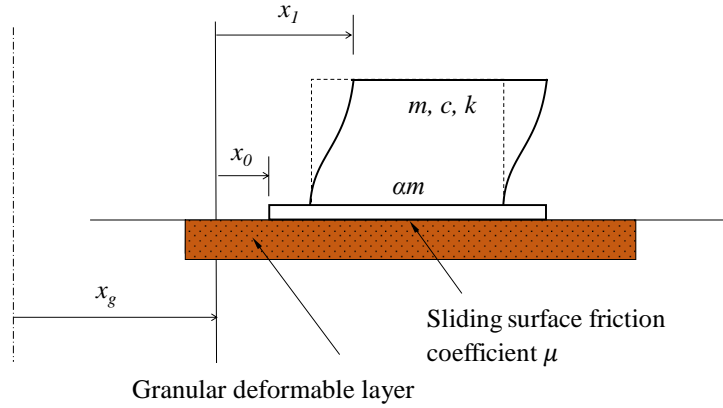

Fig. 1. Modelling of a flexible structure founded on a deformable granular layer.

As shown in Fig. 1, x_1 represents the relative displacement of the structure with primary modal mass m and elastic stiffness k with respect to the ground and x_0 denotes the relative displacement of the rigid base with mass αm with respect to the ground. The horizontal ground displacement is given by x_g. The viscous modal damping coefficient of the structure is denoted as c. The dynamic equilibrium of motion for this system gives:

$$m\left(\ddot{x}_1 + \ddot{x}_g\right) + c\left(\dot{x}_1 - \dot{x}_0\right) + F_s = 0 \tag{1}$$

$$\alpha m\left(\ddot{x}_0 + \ddot{x}_g\right) - c\left(\dot{x}_1 - \dot{x}_0\right) - F_s + F_b = 0 \tag{2}$$

F_s and F_b represent the elastic restoring force of the isolated structure and the frictional force of the sliding interface, respectively. The following system parameters are introduced:

$$\omega^2 = \frac{k}{m}, \quad T = \frac{2\pi}{\omega}, \ 2\zeta\omega = \frac{c}{m} \tag{3}$$

where k is the elastic stiffness of the structure, ω and T are the fixed-base cyclic frequency and vibration period of the structure, respectively and ζ is the viscous damping ratio of the structure.
The elastic restoring force in the isolated structure is:

$$F_s = k\left(x_1 - x_0\right) \tag{4}$$

The frictional strength of the sliding interface with friction coefficient μ is:

$$F_{b,\max} = (1+\alpha)\mu m g \tag{5}$$

2

The inelastic behavior of the sliding layer is simulated using a Bouc-Wen model (1973). The frictional behavior of a rigid-plastic (Coulomb, 1785) and a deformable granular sliding layer of the same frictional strength $F_{b,max}$ is presented in Fig. 2. The yield displacement of the deformable layer is $u_{y,b}$=1cm.

The isolated structure is assumed to maintain its response in the elastic range. Two different types of structures that are located in Nepal and could be seismically retrofitted using the presented seismic isolation strategy are presented in Fig. 3, 4: One steel- and one masonry one-story school are illustrated.
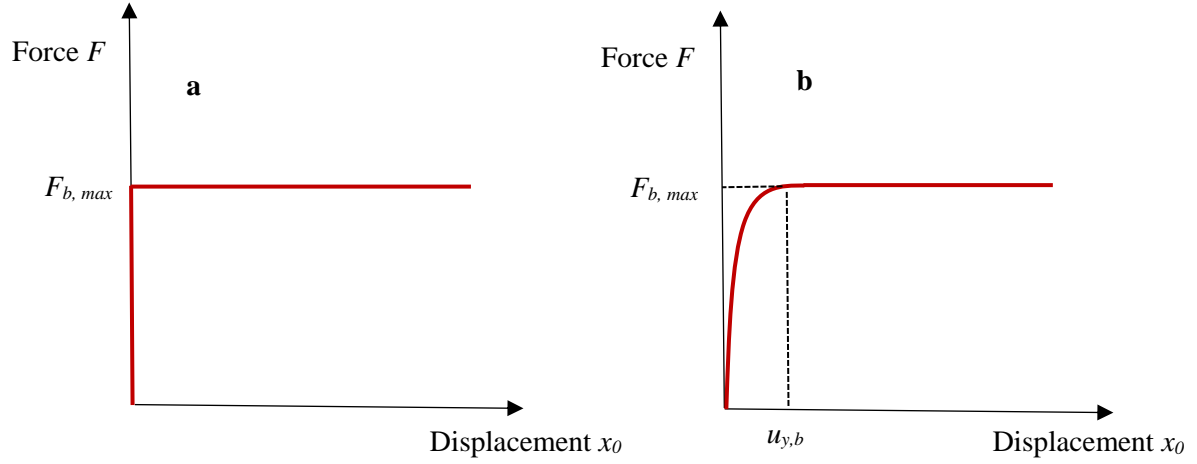

Fig. 2. Modelling of the frictional behaviour of a) a rigid sliding layer; b) a deformable granular sliding layer.

Fig. 3. Picture of a steel school building in Nepal, Copyright: Amar Khamcha, Submitted to the SAFER Project Mobile App.

Fig. 4. Picture of a masonry school building in Nepal, Copyright: Kapil Khatri, Submitted to the SAFER Project Mobile App.

The seismic safety of both types of schools could be substantially improved if they are designed to slide when they are subjected to a strong earthquake ground motion excitation, similar to the destructive ground motions observed during the Gorkha earthquake in 2015. The increase of the safety and resilience of schools in Nepal is the main goal of the SAFER (Seismic Safety and Resilience of Schools in Nepal) Project. This project focuses on the seismic hazard assessment, pre- and post-earthquake structural inspection and seismic retrofitting of school buildings in Nepal. An expert system Mobile App is developed to facilitate the structural inspection of the school buildings and the prioritization of the seismic retrofitting at a community level. An innovative seismic isolation strategy will be proposed for the reduction of seismic damage of the school building inventory.

3. Numerical investigation

The structural system presented in Fig. 1 with vibration period T=0.1s, mass m=25t (α=0.1) and friction coefficient μ=0.4 is excited by a symmetric Ricker (1943) pulse, defined by Eq. 6 and shown in Fig. 5 as the ground motion acceleration $\ddot{u}_g(t)$ with amplitude α_p=0.6g and period T_p=1s. The viscous damping ratio of the structure is 0.05. Two different types of sliding layers are investigated, as shown in Fig. 2: First, a rigid sliding layer (Fig. 2a); second, a deformable granular sliding layer with $u_{y,b}$=1cm (Fig. 2b).

$$\ddot{u}_g(t) = a_p \left(1 - \frac{2\pi^2(t-2)^2}{T_p^2} \right) \exp\left(-\frac{1}{2} \frac{2\pi^2(t-2)^2}{T_p^2} \right) \tag{6}$$
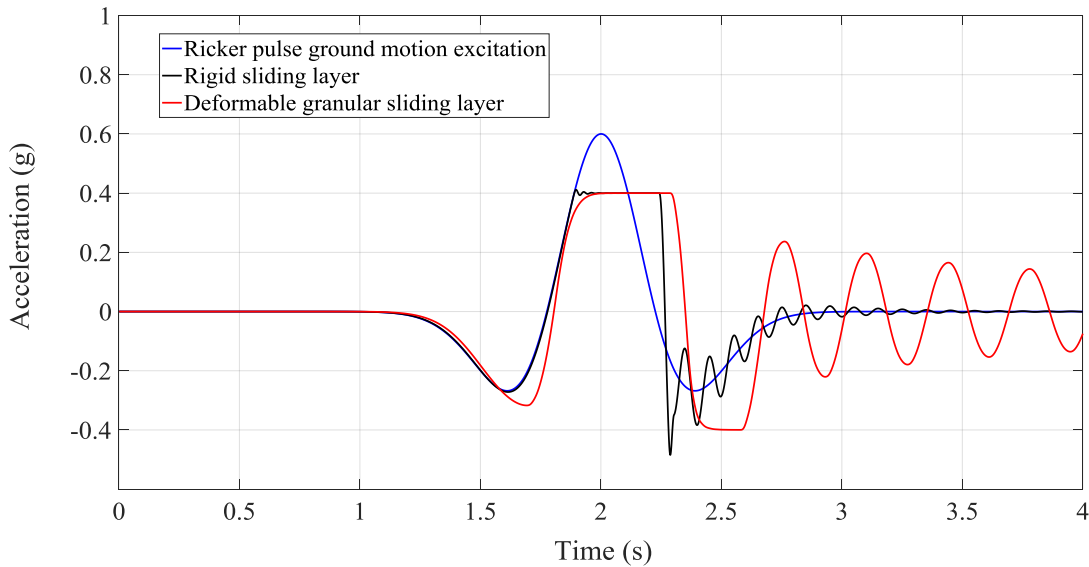

Fig. 5. Acceleration time history response of the structure subjected to analytical Ricker pulse ground motion excitation for two different sliding layer types: a) A rigid sliding layer; b) A deformable sliding layer.

As shown in Fig. 5, the friction of both types of sliding layers was exceeded almost simultaneously, thus facilitating sliding of both structural systems for the selected ground motion excitation. However, the sliding displacement of the deformable layer was significantly higher than the corresponding displacement of the rigid sliding layer, as presented in the hysteretic force-displacement loops and displacement time history responses of both sliding layer types (Fig. 6, 7). Fig. 8 and 9 illustrate the velocity time history response of the sliding layer and the displacement time history response of the structure, respectively, thus presenting a complete quantification of the dynamics of the system subjected to the selected ground motion excitation.
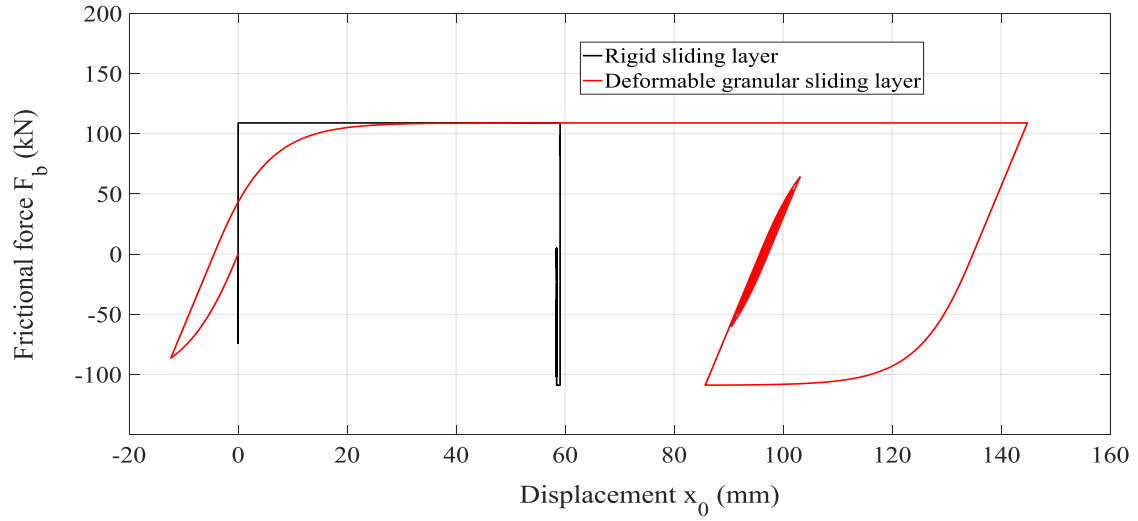
Fig. 6. Hysteretic force-displacement loop of the sliding layer subjected to analytical Ricker pulse ground motion excitation for two different sliding layer types a) A rigid sliding layer b) A deformable sliding layer.
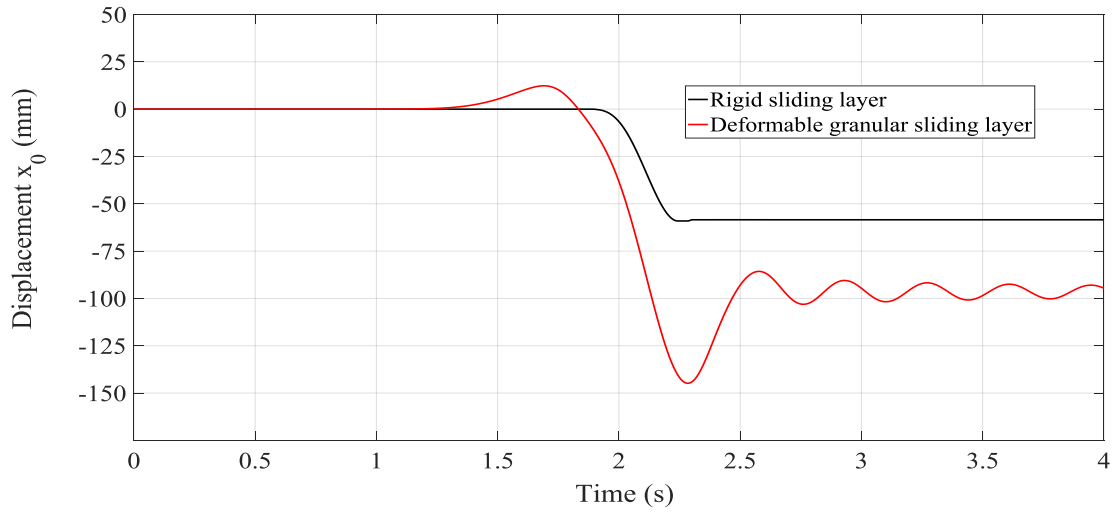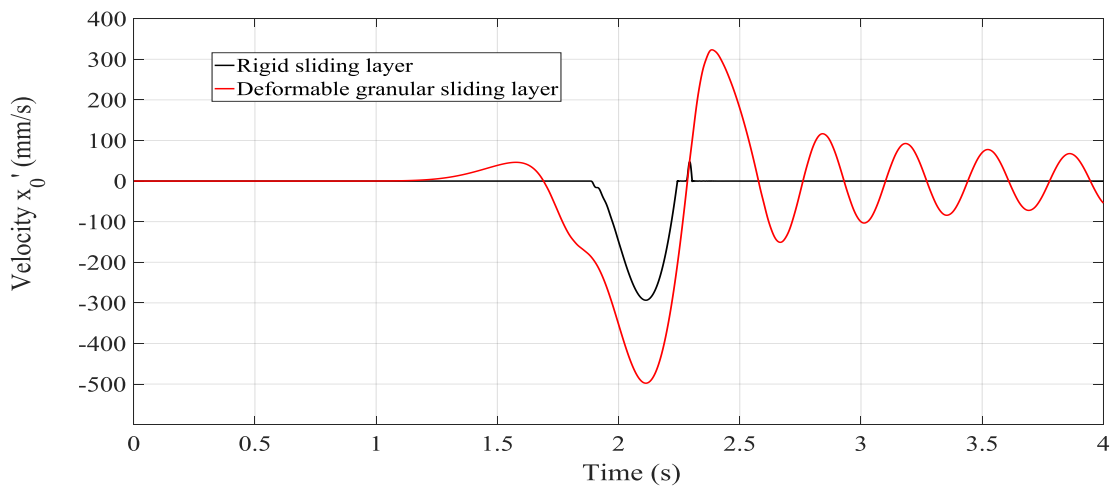

Fig. 7. Displacement time history response of the sliding layer subjected to analytical Ricker pulse ground motion excitation for two different sliding layer types: a) A rigid sliding layer b) A deformable sliding layer.

Fig. 8. Velocity time history response of the sliding layer subjected to analytical Ricker pulse ground motion excitation for two different sliding layer types: a) A rigid sliding layer b) A deformable sliding layer.
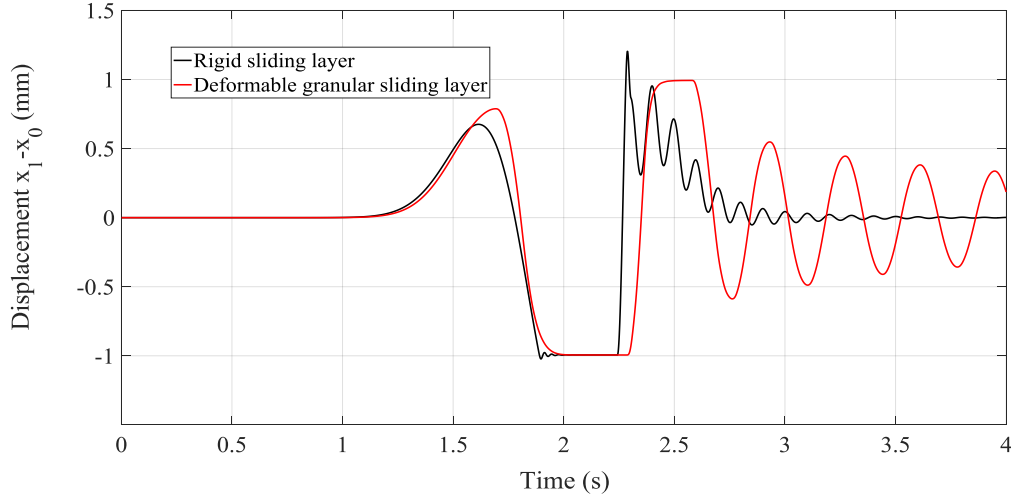
Fig. 9. Displacement time history response of the structure subjected to analytical Ricker pulse ground motion for two different sliding layer types: a) A rigid sliding layer b) A deformable sliding layer.

The main difference in the sliding response of the two different sliding layers is observed in Fig. 8: The deformable sliding layer does acquire a remarkable velocity before sliding due to its flexibility, thus leading to an increased sliding displacement response compared to the rigid sliding layer (Fig. 6, 7), which does not deform before sliding. The increased sliding displacement of the deformable layer has a favourable effect on the response of the isolated structure: The structure that is founded on the deformable sliding layer is subjected to lower acceleration (Fig. 5) and displacement values (Fig. 9). Notably, the energy dissipation that is associated with the increased activation of the deformable sliding layer reduces the deformation of the isolated structure, thus protecting it from seismic damage. The quantification of this seismic damage cannot be performed with the present model which considers the structure to maintain its response in the elastic range and is beyond the scope of this paper.

Fig. 10 illustrates the beneficial role of a deformable sliding layer towards reducing the acceleration of the superstructure for varying Ricker ground motion amplitudes a_p and varying vibration period ratios T/T_p compared to the rigid sliding layer case, presented in Fig. 11.
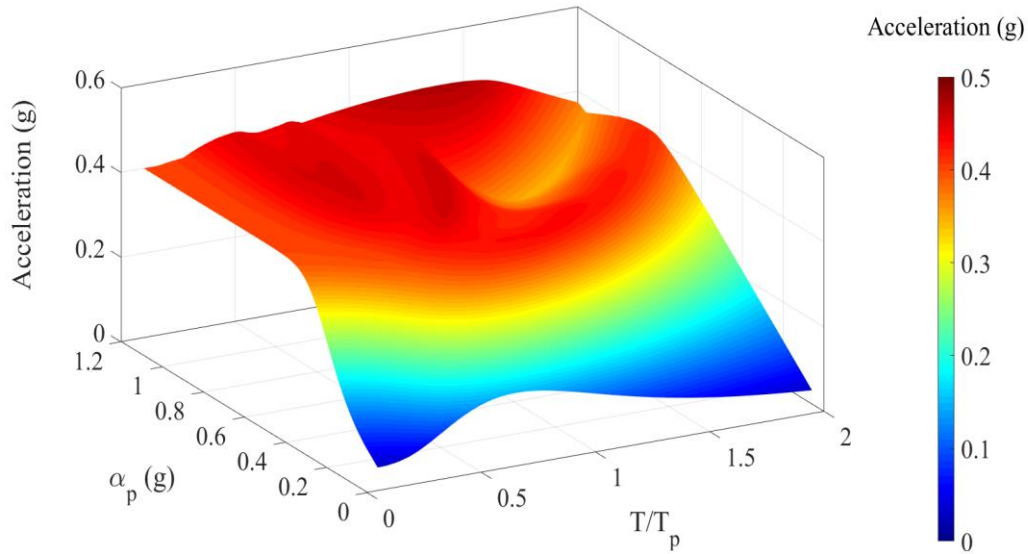

Fig. 10. Maximum acceleration values of the structure (in g) subjected to analytical Ricker pulse ground motion with varying a_p (g) and for different vibration period ratios T/T_p for a deformable granular sliding layer.
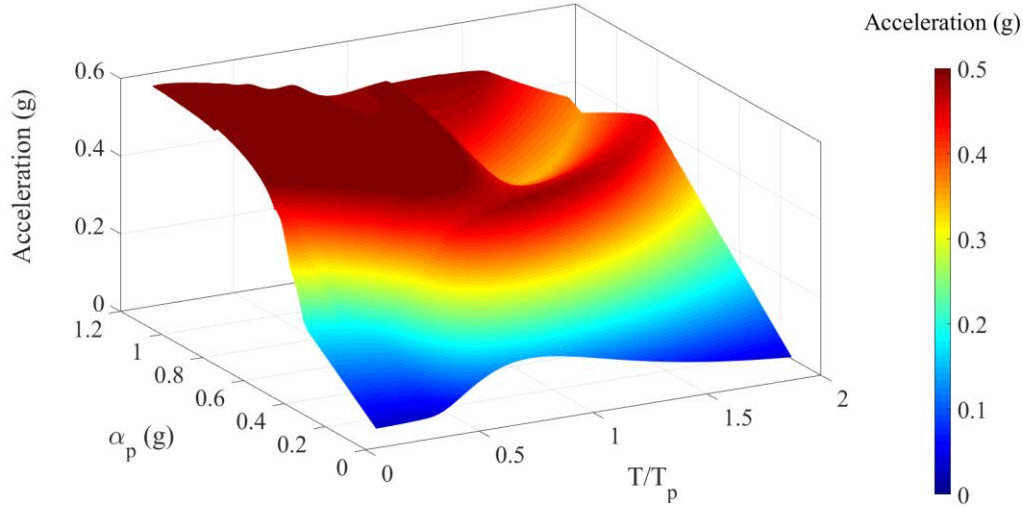
Fig. 11. Maximum acceleration values of the structure (in g) subjected to analytical Ricker pulse ground motion with varying a_p (g) and for different vibration period ratios T/T_p for a rigid sliding layer.

As shown in the figures presented above, the maximum acceleration observed for the rigid sliding layer case is higher than the one corresponding to the deformable layer case for high amplitude values $a_p > 0.4g$ and in the low vibration period range ($T/T_p < 0.5$), representing stiff structures excited by long-period ground motion excitation. In this period range, the deformable sliding layer is characterized by higher velocity before sliding, thus leading to higher sliding displacement values, shown in Fig. 12, 13. On the contrary, the sliding displacement response of both sliding layer types is substantially decreased for higher vibration ratios T/T_p. In this vibration period range, the lower acceleration (Fig. 8, 9) and the force transmitted to the sliding layer from the flexible superstructure inhibits the exceedance of the friction of the sliding layer and the manifestation of sliding response. The direct outcome of this reduced seismic energy dissipation on the sliding layer in this vibration period range is the increased deformation of the isolated structure for both sliding layer types shown in Fig. 14 and 15, which is usually associated with seismic damage. For low amplitude values $a_p < 0.4g$, the friction of the sliding layer is not exceeded and the maximum acceleration response is observed as expected for the case of resonance between the period of the excitation and the vibration period of the superstructure ($T/T_p = 1$).
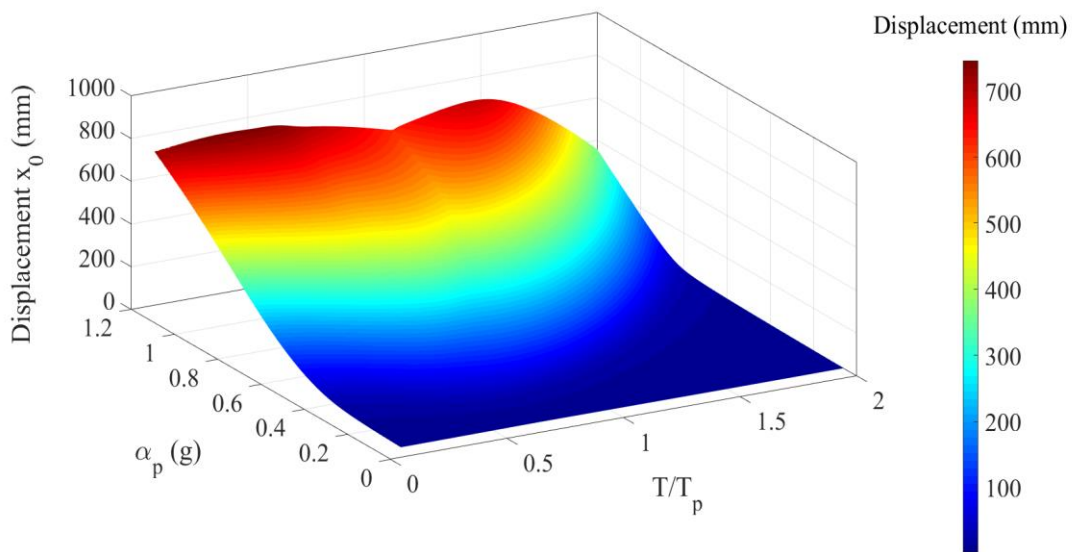

Fig. 12. Maximum displacement values of the sliding layer (in mm) subjected to analytical Ricker pulse ground motion with varying a_p (g) and for different vibration period ratios T/T_p for a deformable granular sliding layer.
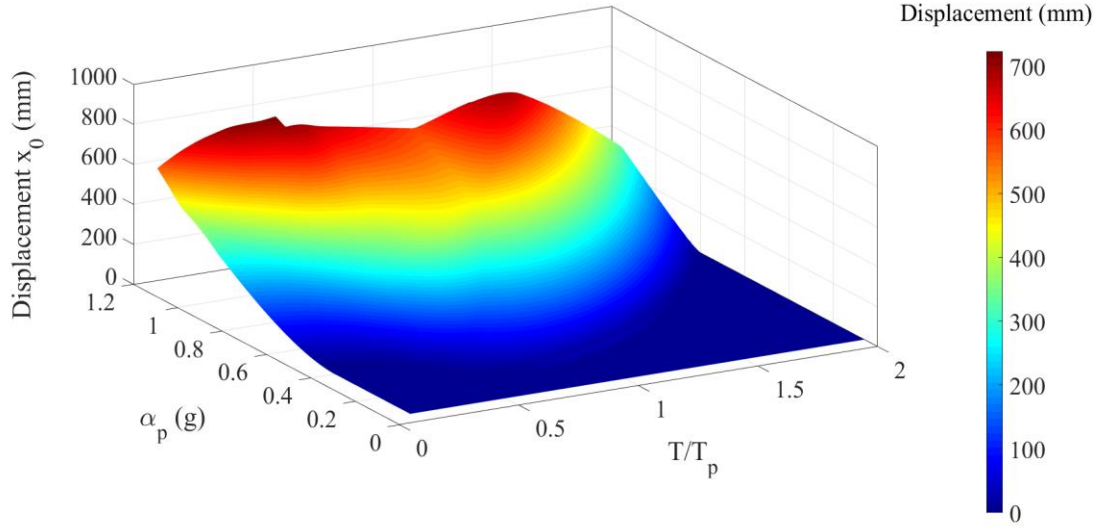
Fig. 13. Maximum displacement values of the sliding layer (in mm) subjected to analytical Ricker pulse ground motion with varying a_p (g) and for different vibration period ratios T/T_p for a rigid sliding layer.

Fig. 14. Maximum displacement values of the structure (in mm) subjected to analytical Ricker pulse ground motion with varying a_p (g) and for different vibration period ratios T/T_p for a deformable granular sliding layer.

Fig. 15. Maximum displacement values of the structure (in mm) subjected to analytical Ricker pulse ground motion with varying a_p (g) and for different vibration period ratios T/T_p for a rigid sliding layer.
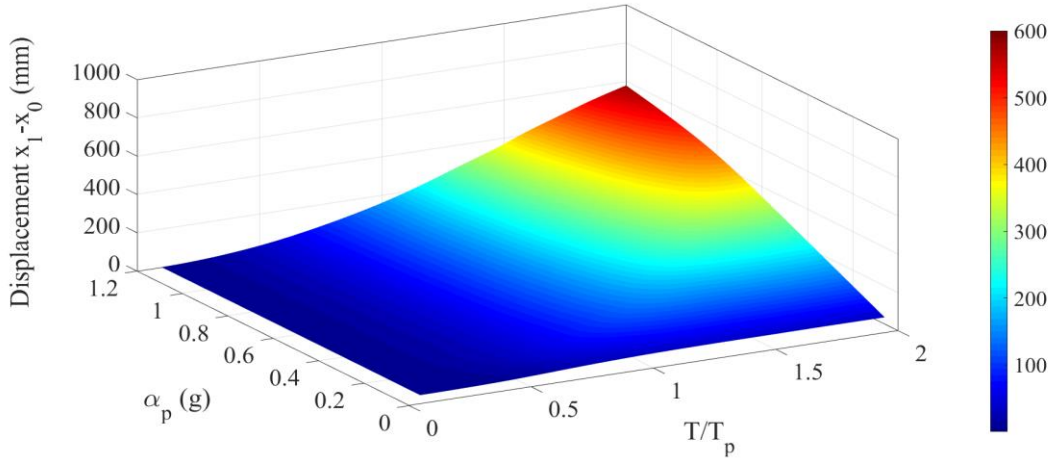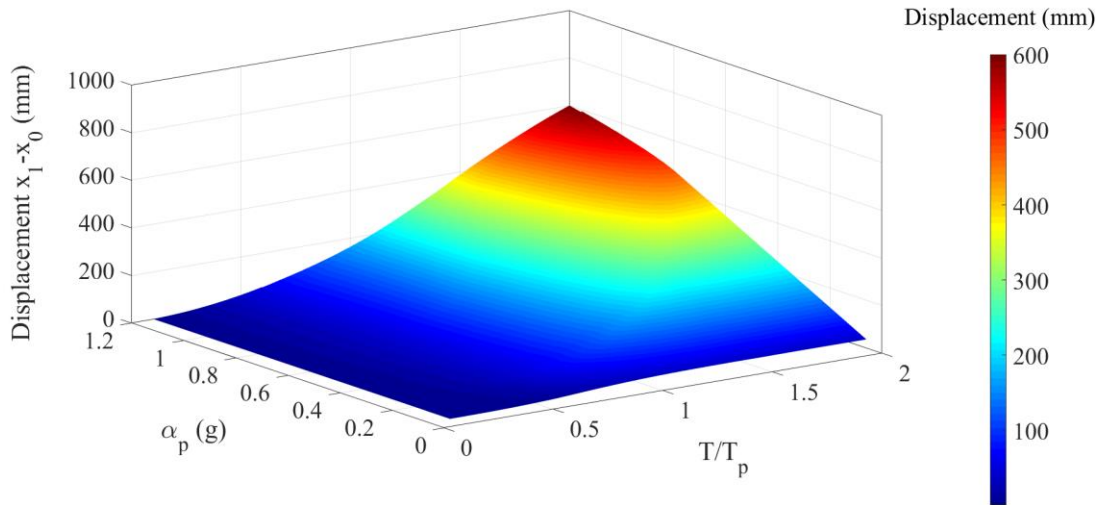
The favourable role of the deformable granular sliding layer towards the reduction of the acceleration response of the seismically isolated structure is shown in Fig. 16: The seismically isolated structure is excited by the 1976 Gazli KAR000 ground motion record, obtained from the PEER ground motion database (2014). As shown in the figure, the decrease of the maximum acceleration due to the action of the deformable layer approaches 30%, while the maximum sliding displacement of the layer is kept within reasonable limits (Fig. 17).
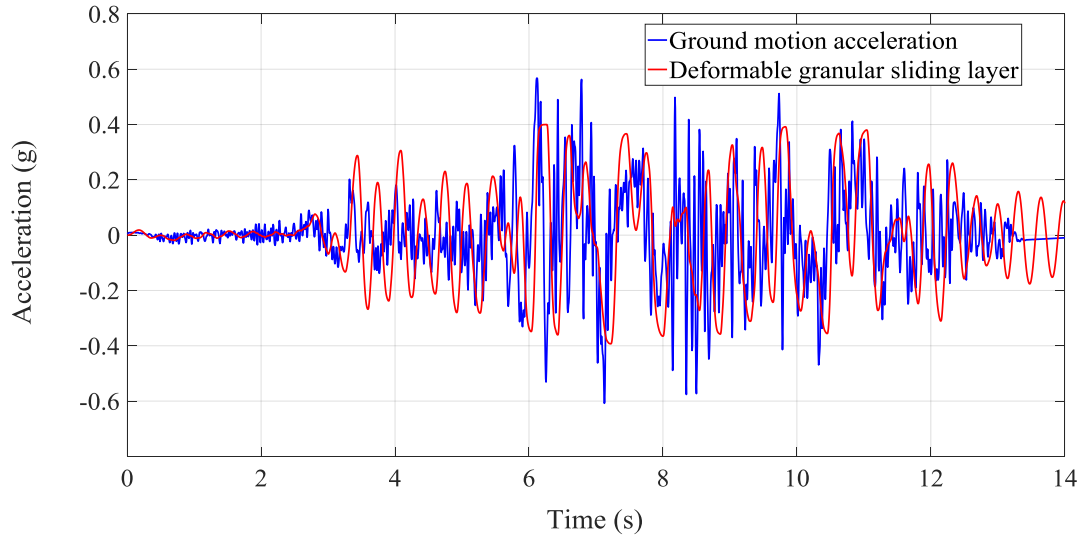

Fig. 16. Acceleration time history response of the structure subjected to the 1976 Gazli ground motion excitation for the case of a deformable sliding layer.
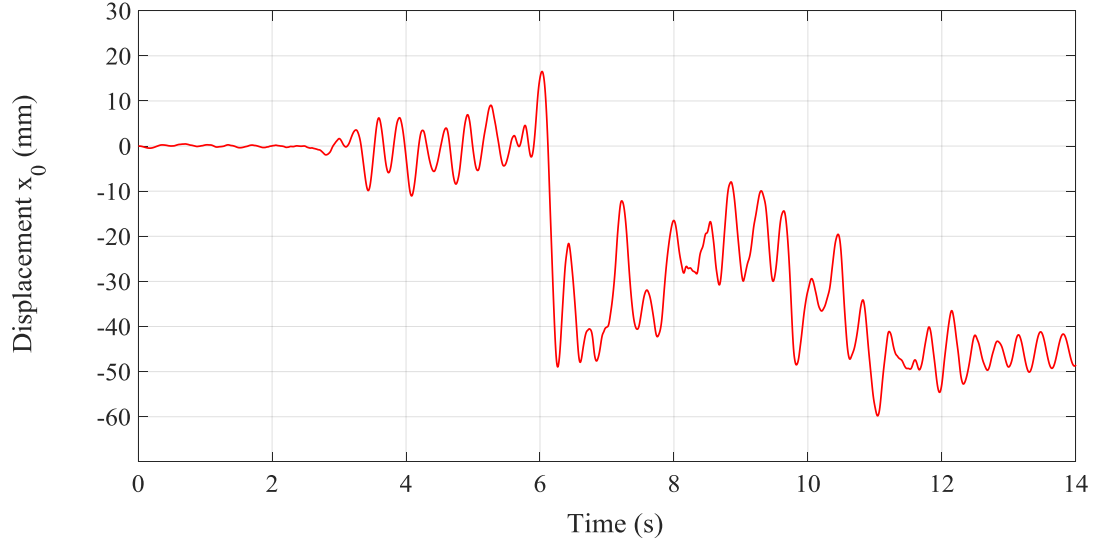

Fig. 17. Displacement time history response of the sliding layer subjected to the 1976 Gazli ground motion excitation for the case of a deformable sliding layer.

4. Conclusions

This study investigates the effect of the use of a deformable granular sliding layer on the seismic response of an isolated structure compared to a rigid sliding layer, which does not deform before sliding. The main reason behind this investigation is the potential design of seismically isolated structures using granular deformable materials, aligned with the goals of the SAFER Project presented in Section 2.

A two-degree-of-freedom model of an isolated structure was subjected to an analytical Ricker pulse ground motion excitation with amplitude a_p=0.6g and period T_p=1s. The sliding response of the deformable sliding layer subjected to this ground motion excitation was substantially higher than the one corresponding to the rigid sliding layer due to the obtained velocity during the oscillation phase of the deformable sliding layer before the initiation of sliding. The increased energy dissipation of the deformable sliding layer that emerged from its sliding response lead to a significant reduction of the acceleration of the isolated structure.

The trends obtained for the aforementioned ground motion excitation were generalized for a wide range of Ricker pulse ground motion amplitudes a_p and ratios T/T_p representing the normalized fixed-base period of the isolated structure to the period of the Ricker pulse ground motion excitation. The beneficial role of the use of a deformable sliding layer for ground motion amplitudes higher than the friction coefficient of the sliding layer and low ratios T/T_p was illustrated: Stiff, seismically isolated structures excited by long-period ground motion excitation are expected to be subjected to lower acceleration values and thus lower seismic forces if the chosen sliding layer manifests deformability before sliding. The design implication of this conclusion is the potential reduction of seismic damage of structures seismically isolated using a deformable sliding granular material. However, the quantification of the seismic damage associated with this response cannot be performed with the model presented in this paper, which considers the structure to remain elastic for the selected ground motion excitation ensemble.

References

Castaldo, P. & Ripani, M. (2016) Optimal design of friction pendulum system properties for isolated structures considering different soil conditions. *Soil Dynamics and Earthquake Engineering*, 90, 74–87.

Coulomb, C. (1785) Theorie des machines simples, en ayant egard au frottement de leurs parties. *Mem Differ Equ Math Phys*, 161–342.

Hill, J. M., & Zheng, X. M. (1996) Dilatant double shearing theory applied to granular chute flow. *Acta Mechanica*, 118, 97-108.

Kulkarni, J. A., & Jangid, R. S. (2003) Effects of superstructure flexibility on the response of base-isolated structures. *Shock and Vibration*, 26, 1–13.

Mostaghel, N., Hejazi, M., & Tanbakuchi, J. (1983a) Response of sliding structures to harmonic support motion. *Earthquake engineering and structural dynamics*, 11(3), 355-366.

Mostaghel, N., & Tanbakuchi, J. (1983b) Response of Sliding Structures to Earthquake Support Motion. *Earthquake Engineering and Structural Dynamics*, 729-748.

Nagarajaiah, S., Reinhorn, A. M., & Constantinou, M. C. (1991) Nonlinear dynamic analysis of 3-D-Base-Isolated stuctures. *Journal of Structural Engineering*, 14, 543-557.

PEER NGA Strong Motion Database (2014) Pacific Earthquake Engineering Research Center, University of California, Berkeley.

Ricker N (1943) Further developments in the wavelet theory of seismogram structure. *Bulletin of the Seismological Society of America*, 33, 197-228.

Tsiavos, A., Mackie, K. R., Vassiliou, M., & Stojadinovic B. (2017) Dynamics of inelastic base-isolated structures subjected to recorded ground motions. *Bulletin of Earthquake Engineering*, 15(4), 1807-1830.

Tsiavos, A., & Stojadinović, B. (2018) Constant yield displacement procedure for seismic evaluation of existing structures. *Bulletin of Earthquake Engineering*, https://doi.org/10.1007/s10518-018-00532-w

Vassiliou, M. F., Tsiavos, A., & Stojadinovic, B. (2013) Dynamics of inelastic base isolated structures subjected to analytical pulse ground motions. *Earthquake Engineering and Structural Dynamics*, 42(14), 2043–2060.

Yaghmaei-Sabegh, S., Safari, S. & Ghayouri, K. A. (2018) Estimation of inelastic displacement ratio for base-isolated structures. *Earthquake Engineering & Structural Dynamics*, 47(3), 634– 659.

Wen, Y.K. (1975) Approximate method for nonlinear random vibration. *Journal of Engineering Mechanics Division (ASCE)*, 101(4), 389–401.

Westermo, B., & Udwadia, F. (1983) Periodic response of a sliding oscillator system to harmonic excitation. *Earthquake engineering and structural dynamics*, 11, 135-146.